Computers and Concrete, *Vol. 19, No. 5 (2017) 545-553*
DOI: https://doi.org/10.12989/cac.2017.19.5.545

Simplified P-M interaction curve model for reinforced concrete columns exposed to standard fire

Deuck Hang Lee[1a], Na-Rae Cheon[2b], Minsu Kim[1c], Jungmin Lee[1c], Jae-Yuel Oh[1d] and Kang Su Kim[*1]

[1]*Department of Architectural Engineering, University of Seoul, 163 Seoulsiripdae-ro, Dongdaemun-gu, 02504, Seoul, Republic of Korea*
[2]*Metallic Materials and Mechanical Engineering Team, Korea Testing & Research Institute, 98 Gyoyukwon-ro, Gwacheon-si, 13810, Gyeonggi-do, Republic of Korea*

(Received January 8, 2017, Revised February 2, 2017, Accepted February 15, 2017)

Abstract. In the authors' previous study, an axial force-flexural moment (P-M) interaction curve model was proposed to evaluate fire-resisting performances of reinforced concrete (RC) column members. The proposed method appeared to properly consider the axial and flexural strength degradations including the secondary moment effects in RC columns due to fire damage. However, the detailed P-M interaction curve model proposed in the authors' previous study requires somewhat complex computational procedures and iterative calculations, which makes it difficult to be used for practical design in its current form. Thus, the aim of this study was to develop a simplified P-M interaction curve model of RC columns exposed to fire considering the effects of fire damage on the material performances and magnitudes of secondary moments. The simplified P-M interaction model proposed in this study was verified using 66 column fire test results collected from literature, and the verification results showed that the proposed simplified method can provide an adequate analysis accuracy of the failure loads and fire-resisting times of the RC column specimens.

Keywords: reinforce concrete column; simplified; fire resistance; P-M interaction curve; secondary moment; slenderness ratio

1. Introduction

It is difficult to accurately evaluate the fire-resisting performance of RC column members exposed to fire due to complicated temperature distributions, material nonlinearities, slenderness effect, and loss of cross-section caused by fire damage including spalling (Han *et al*. 2009, Rodrigues *et al*. 2010, Raut and Kodur 2011, Kodur *et al*. 2013, Tan and Tang 2004). In the authors' previous study (Kang *et al*. 2017), a detailed fire performance evaluation method of RC columns exposed to the standard fire (ISO834 1999) was proposed based on the axial force-flexural moment (P-M) interaction curve approach, in which the effect of the secondary moment (P-δ effect) exposed to fire was considered in a reasonable manner. In the proposed detailed P-M interaction, the axial strengths of the RC columns were limited by Rankine load to consider the uncertainties in their strength degradation due to unexpected loads, construction errors, etc (Rankine 1908). The detailed P-M interaction curve model, however, requires quite a complex computational procedure and iterative calculations, and thus, it is difficult to be used for practical design purpose. In this study, a simplified P-M interaction curve model was proposed for an easy application in the practical design of RC columns against fire, and its accuracy was also verified in detail by comparing analysis results with test results collected from literature (Wang *et al*. 2012, Yeo 2012, Tan and Yao 2003, Lie and Woolerton 1988).

∗Corresponding author, Professor
E-mail: kangkim@uos.ac.kr
[a]Research Professor
[b]Researcher
[c]Graduate Student
[d]Ph.D. Candidate

2. Simplified model

As shown in Fig. 1, Choi *et al*. (2006) simplified the P-M interaction curve of a concrete-filled tube (CFT) column at an ambient temperature using a bilinear curve with a balanced failure point. To apply this approach to slender RC columns, the secondary moment effect needs to be considered in the analysis. In particular, for RC columns exposed to fire, the slenderness effect (so-called P-δ effect) is more significant than that at a room temperature because of the cross-section loss caused by the fire damage. Thus, the secondary moment effect should be considered in the fire resistance design of RC columns (Kang *et al*. 2017, Yeo 2012). This study, therefore, aimed at deriving a simplified P-M interaction curve model considering the effects of secondary moment as well as the fire damage so that it can be utilized in the practical fire resistance design of RC columns.

2.1 Proposed simplified method

In the simplified P-M interaction curve model of a

Copyright © 2017 Techno-Press, Ltd.

ISSN: 1598-8198 (Print), 1598-818X (Online)

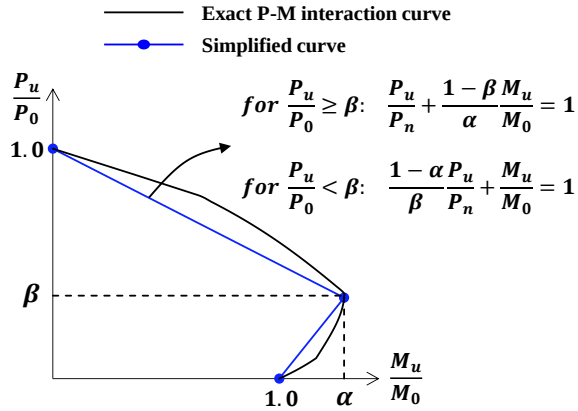

Fig. 1 Normalized P-M interaction curve of column (Choi *et al*. 2006)

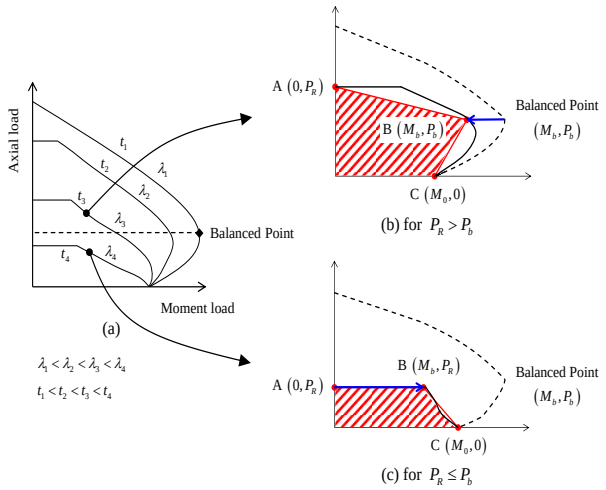

Fig. 2 Concept of proposed simplified approach

concrete-filled tube (CFT) column at an ambient temperature shown in Fig. 1 (Choi *et al*. 2006), the balanced failure point was expressed by two coefficients, α and β. By utilizing these coefficients, the simplified P-M interaction curve of a RC column exposed to fire can be also mathematically expressed, as follows

$$\frac{P_u}{P_0} + \frac{1-\beta}{\alpha}\frac{M_u}{M_0} = 1 \quad \text{for} \frac{P_u}{P_0} \geq \beta \tag{1a}$$

$$\frac{1-\alpha}{\beta}\frac{P_u}{P_0} + \frac{M_u}{M_0} = 1 \quad \text{for} \frac{P_u}{P_0} < \beta \tag{1b}$$

where α and β are the maximum flexural strength at the balanced failure (M_b) normalized by the flexural strength of the column without axial forces (M_0) and the axial compressive strength at the balanced failure (P_b) normalized by the axial capacity of a concentrically-loaded column (P_0), respectively, and P_u and M_u are applied axial loads and moments, respectively. The coefficients α and β in Eq. (1) can be obtained from parametric analyses considering the major influential factors (Choi *et al*. 2006, Choi *et al*. 2008).

As explained in the previous study (Kang *et al*. 2017), the shape of the P-M interaction curve of an RC column significantly varies depending on the effective slenderness ratio and the fire exposure time, i.e., the fire damage. Fig. 2(a) shows the P-M interaction curves of typical RC columns according to the effective slenderness ratios and the fire exposure time. As shown in Fig. 2(b) and (c), the interaction curves can be divided into two types depending on the shapes of the curves. For a column member with a low slenderness ratio and a short fire exposure time, as shown in Fig. 2(b), its P-M curve shape remains basically similar to that at an ambient temperature condition, but its area inside the curve (or curve size) reduces. In addition, the ultimate axial capacity of a concentrically-loaded column limited by Rankine load (P_R) is still larger than the axial compressive strength at the balanced failure (P_b), i.e., $P_R > P_b$. In contrast, for a column member with a high slenderness ratio and a long fire exposure time, as shown in Fig. 2(c), its flexural strength drastically decreases, and its curve shape almost turns into a trapezoid, at which P_R is typically lower than P_b, i.e., $P_R < P_b$. In short, the shape of the P-M interaction curve can be classified into two types depending on the relative magnitude of P_b and P_R. The ultimate axial capacity of a concentrically-loaded column limited by Rankine load (P_R) can be calculated (Kang *et al*. 2017, Yao and Tan 2009, Hu *et al*. 2015, Tan and Tang 2004, Yao *et al*. 2008), as follows

$$\frac{1}{P_R} = \frac{1}{P_0} + \frac{1}{P_e} \tag{2a}$$

$$P_e = \frac{\pi^2 (EI)_{eff}}{(kL)^2} \tag{2b}$$

where P_ε is Euler's buckling load, kL is the effective length of the column, and $(EI)_{eff}$ is the effective flexural stiffness of the column.

As shown in Fig. 2(b) and (c), the simplified bilinear P-M interaction curve can be fully defined by three points: A, B, and C. The points A and C are the axial capacity of a concentrically-loaded column (P_0) without moments and the flexural moment capacity of an RC column without axial loads (M_0), respectively. These values can be easily estimated based on the 500℃ isotherm method as explained in the authors' previous study (Kang *et al*. 2017) and the Appendix A of this study as well. Point B is the balanced point, and the simplified P-M interaction curve can be drawn by connecting the points A, B, and C. The shape of the P-M interaction curve thus depends on the position of the point B. Any combinations of an axial load (P) and a moment (M) included in the area inside the original P-M interaction curve can be resisted by the RC column without failure and thus can be selected for the fire resistance design. Thus, as the simplified P-M interaction curve includes more of the area inside the original P-M curve, the accuracy of the simplified P-M interaction curve can be increased. In this study, the point B is determined depending on the relative magnitude of the axial strength limited by Rankine load (P_R) and that at a balanced failure point (P_b). As shown in Fig. 2(b), when the axial strength limited by Rankine load (P_R) is greater than the axial strength at a balanced failure point (P_b), i.e., $P_R > P_b$, the flexural moment capacity of the RC column exposed to fire

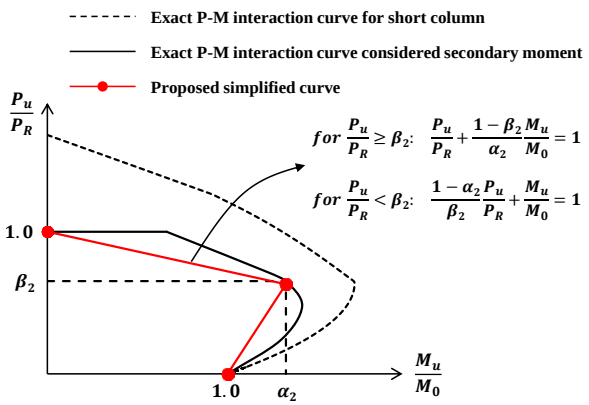

(a) $P_R > P_b(=\beta P_0)$

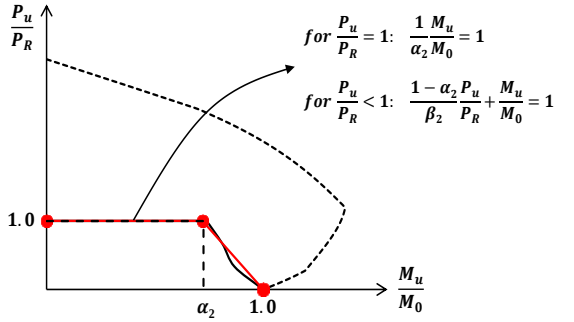

(b) $P_R \leq P_b(=\beta P_0)$

Fig. 3 Proposed simplified approach considering secondary moment effect

at a balanced failure point (M_b) is taken as the point B. Also, as shown in Fig. 2(c), when $P_R \leq P_b$, the maximum flexural capacity of the column section at Rankine load (M_R) is defined as the point B.

Fig. 3 shows the P-M interaction curve normalized by the axial strength limited by Rankine load (P_R) and the flexural strength of the column without axial forces (M_0), in which the idealized balanced failure point (i.e., point B) was expressed using coefficients α_2 and β_2. Thus, when $P_r > P_b$ ($=\beta P_0$), the normalized P-M interaction curve can be expressed, as follows

$$\frac{P_u}{P_R} + \frac{1-\beta_2}{\alpha_2}\frac{M_u}{M_0} = 1 \quad \text{for} \frac{P_u}{P_R} \geq \beta_2 \tag{3a}$$

$$\frac{1-\alpha_2}{\beta_2}\frac{P_u}{P_R} + \frac{M_u}{M_0} = 1 \quad \text{for} \frac{P_u}{P_R} < \beta_2 \tag{3b}$$

Also, when $P_R \leq P_b(=\beta P_0)$, the normalized P-M interaction curve can also be expressed, as follows

$$\frac{1}{\alpha_2}\frac{M_u}{M_0} = 1 \quad \text{for} \frac{P_u}{P_R} = 1 \tag{4a}$$

$$\frac{1-\alpha_2}{\beta_2}\frac{P_u}{P_R} + \frac{M_u}{M_0} = 1 \quad \text{for} \frac{P_u}{P_R} < 1 \tag{4b}$$

where α_2 and β_2 are the coefficients for the balanced failure point in the normalized P-M interaction curve. The coefficients α_2 and β_2 as well as α and β can be determined

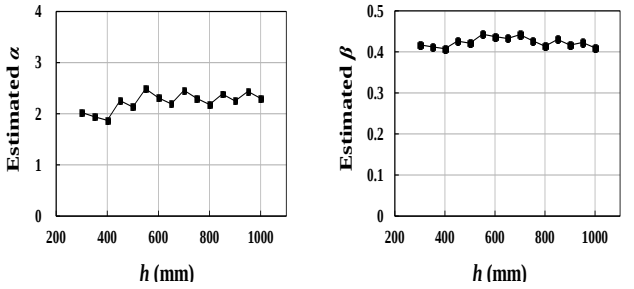

(a) Wind speed profile

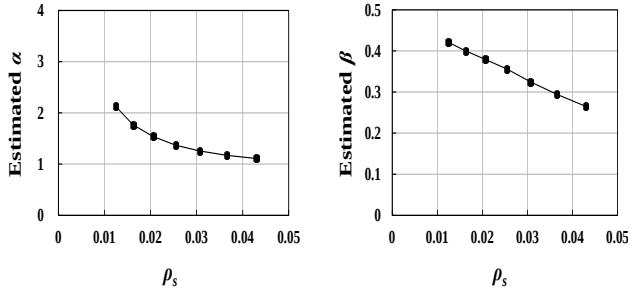

(b) Effect of longitudinal reinforcement ratio

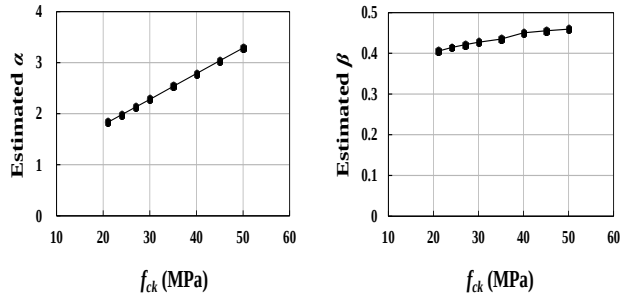

(c) Effect of compressive strength of concrete

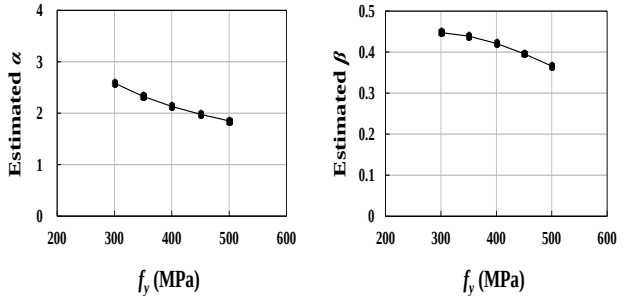

(d) Effect of yield strength of steel

Fig. 4 Parametric study of detailed analysis model with various influential factors

from regression analysis based on parametric study results as explained in the following section.

2.2 Parametric study to determine the balanced point factors

As afore-mentioned, the coefficient α is the maximum flexural strength at the balanced failure normalized by the flexural strength of the column without axial forces (M_b/M_0), and β is the axial compressive strength at the balanced failure normalized by the axial capacity of a concentrically-loaded column (P_b/P_0). In this study, parametric studies were performed to determine the factors α and β, where the key variables were the area of gross

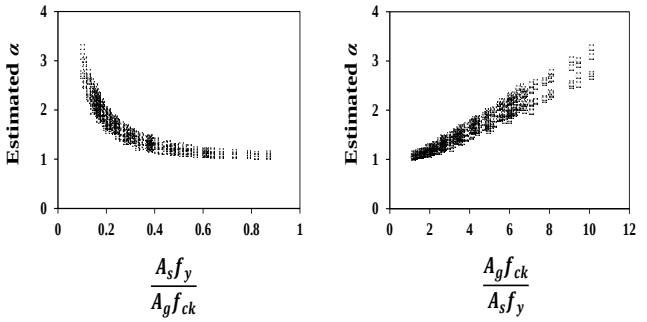

(a) Distribution of α

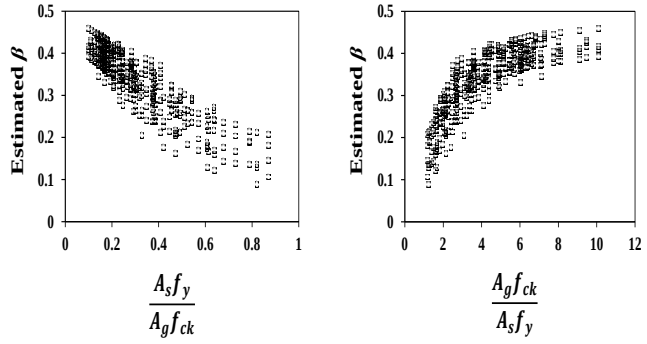

(b) Distribution of β

Fig. 5 Parametric study results for determination of α and β

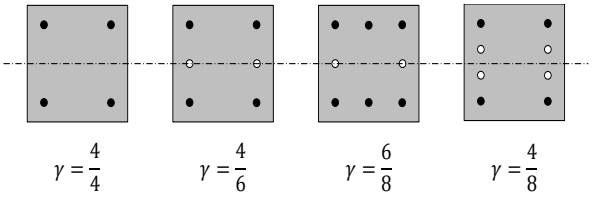

Fig. 6 Reinforcement arrangement factor (γ) for various reinforcement details

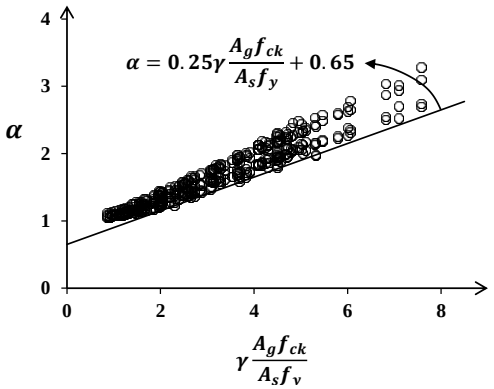

(a) Approximation of α with detail analysis results

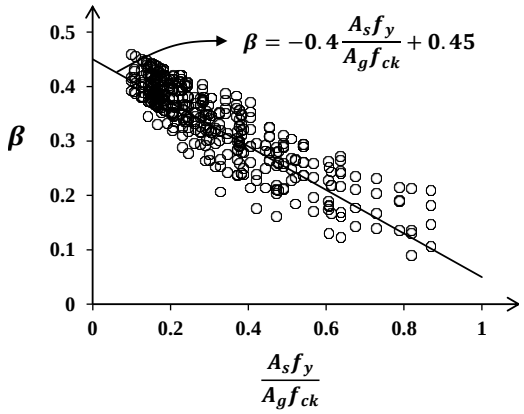

(b) Approximation of β with detail analysis results

Fig. 7 Determination of α and β as linear functions based on parametric analysis results

section (A_g), the longitudinal tension reinforcement ratio (ρ_s=A_s/bd), the compressive strength of concrete at an ambient temperature (f_{ck}), and the yield strength of the reinforcement (f_y). The parametric study conducted in this study included most of the column cross-sectional details that have been frequently used in practice. The range of the cross-sectional height (h) considered in the parametric analyses were from 300 mm to 1000 mm, the reinforcement ratio (ρ_s) ranged from 1.0% to 4.0%, the compressive strength of concrete (f_{ck}) ranged from 20 MPa to 50 MPa, and the yield strength of reinforcement at an ambient temperature (f_y) ranged from 300 MPa to 500 MPa.

Fig. 4 shows the analysis results of the parametric study using the detailed P-M interaction model proposed in the authors' previous study (Kang *et al*. 2017) against the aforementioned key influential factors. As the tension reinforcement ratio (ρ_s) and the yield strength of the reinforcement (f_y) increase, α values show a decreasing trend. This is because, as the reinforcement ratio (ρ_s) and the yield strength of the reinforcement (f_y) increase, the flexural strengths of RC sections are typically governed by the compression-controlled behavior, and thus the balanced points move downwards and inwards. In addition, the β values also tend to decrease as the reinforcement ratio (ρ_s) and the yield strength of the reinforcement (f_y) increase. This means that, as the reinforcement ratio (ρ_s) and the yield strength of the reinforcement (f_y) increase, the axial capacity of a concentrically-loaded column (P_0) increases significantly, and thus the difference between P_b and P_0 increases. Based on the analysis results, the axial strength ratio of the reinforcement to the concrete in a RC section, k_s(=$A_s f_y$/$A_g f_{ck}$), was introduced. This strength ratio (k_s) is identical to the tension reinforcement index, ω_s(ω_z=$\rho_s f_y$/f_{ck}), which is one of the indicators of the reinforcing degree in flexure. As shown in Fig. 5, the strength ratio (κ_s) shows a strong correlation with the coefficients α and β. In particular, α values showed a linearly proportional relation with the inverse of κ_s, and β values showed a linear inversely proportional relationship with κ_s. In addition to the tension reinforcement ratio (ρ_s), the flexural strength of RC section and the shape of the P-M interaction curve are significantly affected by the details of reinforcement arrangement (Johnson 2008). Thus, the reinforcement arrangement factor (γ) was introduced in this study, which is the ratio between the sectional area of the extreme tension reinforcement to that of the total reinforcement provided in the RC section. Fig. 6 shows how the values of the coefficient γ can be determined on the RC sections with various reinforcement details.

Based on the parametric analysis results, the coefficients α and β were derived as simple forms of linear equations, in which the reinforcement arrangement factor (γ) was

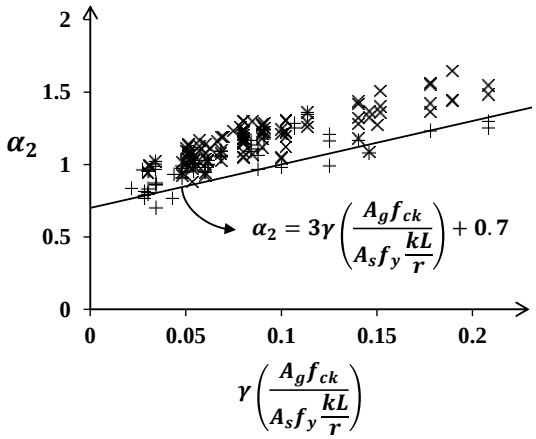

Fig. 8 Determination of α_2 as linear functions based on parametric analysis results

included only in the coefficient α because the γ factor affects the flexural strength only. As shown in Fig. 7(a) and (b), α was determined in a conservative manner while β was obtained in an average sense. The coefficients α and β derived from the regression analysis are, as follows

$$\alpha = 0.25\gamma\frac{A_g f_{ck}}{A_s f_y} + 0.65 \tag{5a}$$

$$\beta = -0.4\frac{A_s f_y}{A_g f_{ck}} + 0.45 \tag{5b}$$

The coefficients α_2 and β_2 define the intermediate point of the simplified P-M interaction curve for the RC column exposed to fire considering the secondary moment proposed in this study. Since β is P_b/P_0 and β_2 is P_b/P_R, β_2 can be estimated by multiplying β with P_0/P_R. In addition, since α_2 indicates the flexural moment strength of the P-M interaction curve considering the secondary moment, the slenderness ratio (λ_s=kL/r) also needs to be considered additionally in determining the coefficient α_2 with the variables used in determining the coefficient α. The flexural moment strength decreases with an increase in the slenderness ratio (λ_s), and thus, λ_s was placed to the denominator of $\gamma A_g f_{ck}/A_s f_y$ in Eq. (5a). As shown in Fig. 8, α_2 showed a proportional relationship with $\gamma A_g f_{ck}/A_s f_y \lambda_s$. For a conservative estimation, in this study, α_2 was determined, as follows

$$\alpha_2 = 3\gamma\frac{A_g f_{ck}}{A_s f_y \lambda_s} + 0.7 \tag{6a}$$

and, as afore-mentioned, β_2 can be calculated, as follows

$$\beta_2 = \beta\frac{P_0}{P_R} \tag{6b}$$

Fig. 9 shows the computational procedures for drawing the simplified P-M interaction curve of an RC column exposed to fire. In addition, Appendix shows the step-by-step calculation process of the P-M interaction curve of an RC column member exposed to fire using the simplified

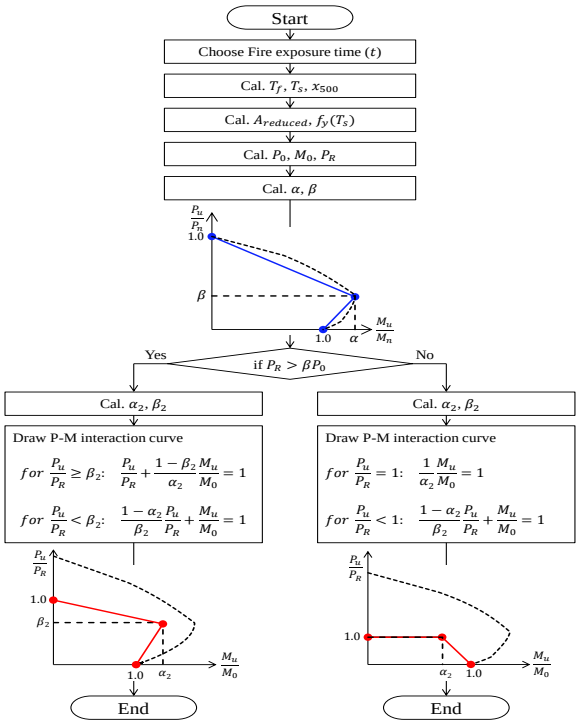

Fig. 9 Computational procedures for estimation of simplified P-M interaction curve

method. By plotting the simplified P-M interaction curve for different fire exposure times (t) according to the procedure proposed in Fig. 9, all the maximum load combinations (P and M) at a required fire-resisting time can be estimated or the fire-resisting time of an RC member subjected to a specific load combination (P and M) can be also estimated without complex fire behavior analysis. In other words, if an engineer estimates the axial load ratio at an ambient temperature (P_u/P_0), which is commonly determined in the structural design process of a column at an ambient temperature, the fire-resisting performance of the column can be easily evaluated without any complex calculation.

2.3 Limitations

This study focused on the fire-resisting performance of RC columns with a rectangular cross-section exposed to fire on four sides of the member. As afore-mentioned, a wide range of the key variables, which may cover most cases used in practice, were considered in the parametric analyses that was performed to determine the important values for the simplified P-M interaction curve of RC columns exposed to fire. However, it should be noted that only the columns with a cover thickness greater than 40 mm were considered in this study according to the requirement on the minimum cover thickness of RC columns specified in the current design code (ACI318-11 2011).

3. Verification

To verify the simplified P-M interaction curve proposed

Table 1 Summary of dimensions and material properties of collected specimens

Investigator(s)	Number of specimen	b or h (mm)	ρ_s (%)	L (m)	f_{ck} (MPa)	f_y (MPa)	c_c (mm)	e (mm)	P_u (MPa)	t (min)
Yeo (2012)	3	250 to 350	2.5 to 4.95	3	24	400	61	0	1225 to 1837	170 to 210
Tan and Yao (2003)	39	200 to 300	2.1 to 3.1	3.8 to 5.8	24.1 to 42.3	418 to 544	30 to 38	0 to 150	122 to 1695	31 to 160
Lie and Woolerton (1988)	24	203 to 406	2.2 to 4.4	3.8	34.2 to 52.9	414 to 444	48 to 64	0 to 44	169 to 2978	146 to 285

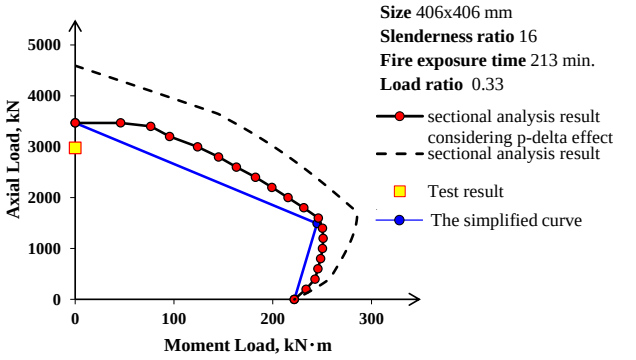

(a) Lie and Woolerton's Specimens 1

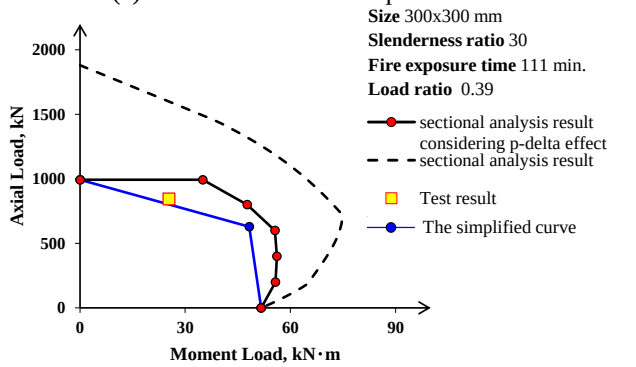

(b) Tan and Yao's Specimen 1

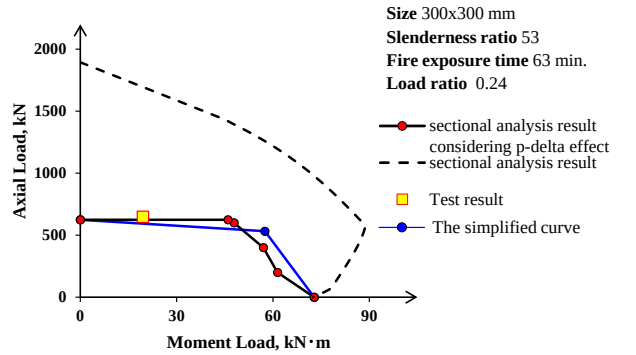

(c) Tan and Yao's Specimen 2

Fig. 10 Verification of simplified P-M interaction model for RC columns with P_R>P_b

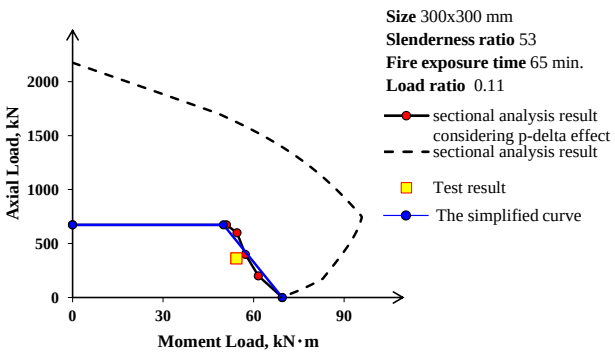

(a) Tan and Yao's Specimen 3

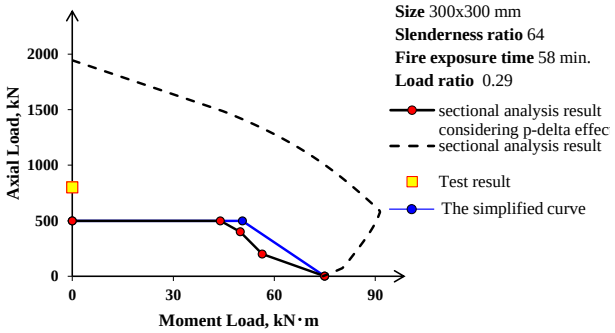

(b) Tan and Yao's Specimen 4

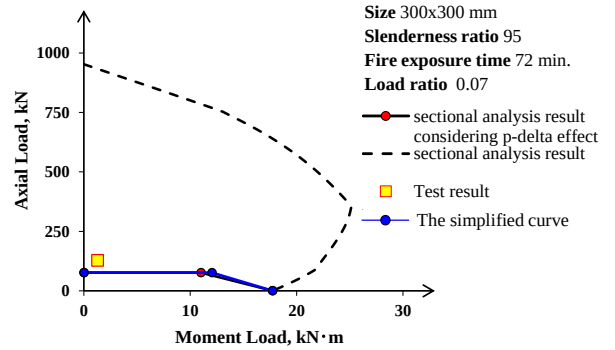

(c) Tan and Yao's Specimen 5

Fig. 11 Verification of simplified P-M interaction model for RC columns with P_R≤P_b

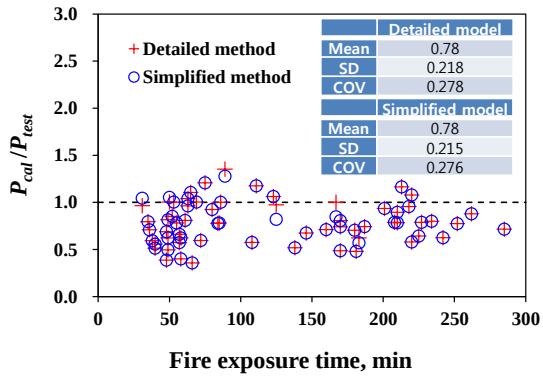

Fig. 12 Comparison of simplified and detailed models with test results

in this study, the fire test results of 66 RC column specimens were collected from previous studies (Lie and Woolerton 1988, Tan and Yao 2003, Yeo 2012). The dimensional details and material properties of the collected test specimens are summarized in Table 1. Figs. 10 and 11 show the analysis results of the collected RC column specimens with P_R greater than P_b, i.e., P_R>P_b, and those with P_R smaller than P_b, i.e., P_R≤P_b, respectively. For the test specimens with different slenderness ratios (λ_s), eccentricities, load ratios at an ambient temperature condition (P_u/P_0), and fire exposure times (t), the simplified P-M interaction curve had very similar curve shapes with those drawn by the detailed analysis model, and the proposed method provided a high level of analysis accuracy

for the fire resistance capacities of test specimens. Fig. 12 shows the axial strength ratios of test results to the results estimated by the proposed method (P_{cal}/P_{test}) according to the fire exposure time, while the analysis results calculated by the detailed model are also included in the figure for comparison purposes. The analysis results provided by the simplified method showed almost the same level of accuracy as those by the detailed analysis model. The simplified model also provided adequately accurate analysis results for the concentrically-loaded specimens as well as the eccentrically-loaded specimens.

4. Conclusions

This study proposed a simplified P-M interaction model, which can be easily applied to fire resistance design of RC columns, modified from the detailed analysis model presented in the authors' previous study. In order to verify the proposed model, the RC column specimens exposed to fire reported in literature were collected, and the test results were compared to those estimated by the proposed method. Based on this study, the following conclusions can be drawn.

• By using the P-M interaction curve model for RC columns exposed to fire, all the maximum load combinations (P and M) at a target fire exposure time required in the performance-based fire design can be estimated, or the maximum fire-resisting time of the RC columns under a specific load combination can be determined without complex iterative calculations.

• The simplified P-M interaction curve approach provided very close curve to that drawn by the detailed analysis model, and the proposed method provided good estimation on the fire resistance capacities of test specimens.

• The simplified model provided adequately accurate analysis results for the concentrically-loaded specimens as well as the eccentrically-loaded specimens.

• By applying the simplified method proposed in this study, RC members can be easily designed to satisfy the fire-resisting performances required by national design provisions.

Acknowledgments

This research was supported by a grant (17AUDP-B100356-03) from Urban Architecture Research Program funded by Ministry of Land, Infrastructure and Transport of Korean government.

References

ACI Committee 318 (2011), *Building Code Requirements for Structural Concrete and Commentary*, Michigan, U.S.A.

Choi, Y.H., Foutch, D.A. and LaFave, J.M. (2006), "New approach to AISC P-M interaction curve for square concrete filled tube (CFT) beam-columns", *Eng. Struct.*, **28**(11), 1586-1598.

Choi, Y.H., Kim, K.S. and Choi, S.M. (2008), "Simplified P-M interaction curve for square steel tube filled with high-strength concrete", *Thin Wall Struct.*, **46**(5), 506-515.

Han, C., Han, M. and Heo, Y. (2009), "Improvement of residual compressive strength and spalling resistance of high-strength RC columns subjected to fire", *Constr. Build. Mater.*, **23**(1), 107-116.

Hu, X., Guo, H. and Yao, Y. (2015), "Interaction approach for concrete filled steel tube columns under fire conditions", *J. Build. Eng.*, **3**, 144-154.

ISO 834 (1999), *Fire-Resistance Tests-Elements of Building Construction-Part 1: General Requirements*, International Organization for Standardization, Geneva, Switzerland.

ISO 834 (1999), *Fire-Resistance Tests-Elements of Building Construction-Part 1: General Requirements*, International Organization for Standardization, Geneva, Switzerland.

Johnson, P. (2008), "P-M characteristics of reinforced concrete sections", M.S. Dissertation, Clemson University, Clemson, U.S.A.

Kang, H., Cheon, N.R., Lee, D.H., Lee, J., Kim, K.S. and Kim, H. Y. (2017), "P-M interaction curve for reinforced concrete column exposed to elevated temperature", *Comput. Concrete*, In Press.

Kang, H., Lee, D.H., Hwang, J.H., Oh, J.Y., Kim, K.S. and Kim, H.Y. (2015), "Structural performances of prestressed composite members with corrugated webs exposed to fire", *Fire Technol.*, **52**(6), 1957-1981.

Kodur, V., Raut, N. and Mao, X. (2013), "Simplified approach for evaluating residual strength of fire-exposed reinforced concrete columns", *Mater. Struct.*, **46**(12), 2059-2075.

Lee, S.J., Lee, D.H., Kim, K.S., Oh, J.Y., Park, M.K. and Yang, I.S. (2013), "Seismic performances of RC columns reinforced with screw ribbed reinforcements connected by mechanical splice", *Comput. Concrete*, **12**(2), 131-149.

Lie, T.T. and Irwin, R.J. (1993), "Method to calculate the fire resistance of reinforced concrete columns with rectangular cross section", *ACI Struct. J.*, **90**(1), 52-60.

Lie, T.T. and Woolerton, J.L. (1988), "Fire resistance of reinforced concrete columns-test results", Internal Report No. 569, National Research Council Canada, Ottawa, Canada.

Rodrigues, J.P.C., Laím, L. and Correia, A.M. (2010), "Behaviour of firber reinforced concrete columns in fire", *Compos. Struct.*, **92**(5), 1263-1268.

Rout, N.K. and Kodur, V.K.R. (2011), "Response of high-strength concrete columns under design fire exposure", *J. Struct. Eng.*, **137**(1), 69-79.

Tan, K.H. and Tang, C.Y. (2004), "Interaction formula for reinforced concrete columns in fire conditions", *ACI Struct. J.*, **101**(1), 19-28.

Tan, K.H. and Yao, Y. (2003), "Fire resistance of four-face heated reinforced concrete columns", *J. Struct. Eng.*, **129**(9), 1220-1229.

Wang, Y., Burgess, I., Wald, F. and Gillie, M. (2012), *Performance-Based Fire Engineering of Structures*, CRC Press, New York, U.S.A.

Yao, Y. and Tan, K.H. (2009), "Extended rankine approach for bi-axially loaded steel columns under natural fire", *Eng. Struct.*, **31**(5), 1024-1031.

Yao, Y., Tan, K.H. and Tang, C.Y. (2008), "The effect of a shear bond in the rankine method for the fire resistance of RC columns", *Eng. Struct.*, **30**(12), 3595-3602.

Yeo, I.H. (2012), "A proposal for load ratio of reinforced concrete column subjected to standard fire", Ph.D. Dissertation, University of Seoul, Seoul, Korea.

CC

Appendix: Application example

The step-by-step calculation procedures for an application of the simplified P-M interaction curve model to a fire-exposed RC column are presented in detail here in this Appendix. This example shows detailed calculations to derive the P-M interaction curve for the No. 1 column specimen reported by Lie and Irwin (1993). The dimensional details and material properties of the specimen are shown in Fig. A1.

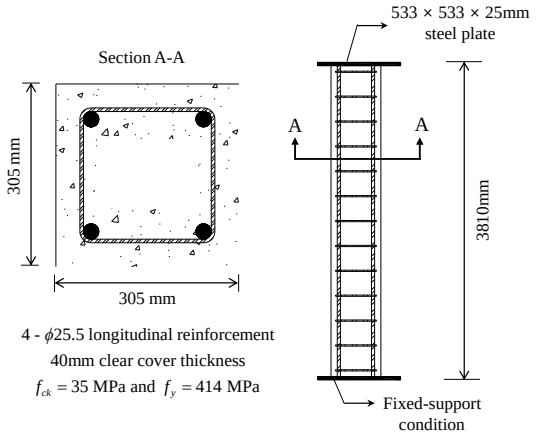

Fig. A1 Dimensions and material properties of the sample RC column

Step 1: Target fire-resisting time

For an example, the target fire-resisting time (t) was selected as three hours (180 minutes).

Step 2: Calculation of the temperatures in the column section

The temperature in the reinforcement (T_s) can be calculated, as follows:

$$T_s = n_x n_w \Delta T_f + 20 = 0.481 \times 0.977 \times 1090 + 20 = 496℃$$

where the increase in the temperature of the fire (ΔT_f) is calculated based on the ISO 834 standard (1999) fire curve, as follows:

$$\Delta T_f = 345 \log(8t+1) = 345 \log(8 \times 180 + 1) = 1090℃$$

In addition, the constants n_x and n_w can be estimated, as follows:

$$n_w = 1 - 0.0616 t^{-0.88} = 1 - 0.0616 \times (180/60)^{-0.88} = 0.977$$

$$n_x = 0.18 \ln \gamma \frac{t}{x^2} - 0.81 = 0.18 \ln \frac{180/60}{(0.04+0.01275)^2} - 0.81 = 0.447$$

Accordingly, the penetration depth to the 500℃ isotherm determined using Wickstrom's equation (x_{500}) is calculated as follows:

$$x_{500} = \left[\frac{t}{\exp\left(4.5 + \frac{480}{0.18 n_w \Delta T_f}\right)} \right]^{0.5} = \left[\frac{180/60}{\exp\left(4.5 + \frac{480}{0.18 \times 0.977 \times 1090}\right)} \right]^{0.5} = 52.2\text{mm}$$

where x_{500}=52.2<(c_c+d_b)=40+12.75=52.75 mm, and the effective cross-section area of concrete is thus calculated based on the 500℃ isotherm method, as follows:

$$A_{reduced} = (b - 2x_{500})(h - 2x_{500}) - A_s = (305 - 2 \times 52.2)^2 - 2042.8 = 38{,}197\text{mm}^2$$

The reduction factors of the yield strength of reinforcing steel and the yield strength of steel at temperature T_s can be calculated, respectively, as follows:

$$K_s(T_s) = K_s(496℃) = 0.57 - 0.13(T - 500)/100 = 0.57 - 0.13(496 - 500)/100 = 0.575$$

$$f_y(T_s) = K_s(T_s) \times f_y = 0.575 \times 414 = 238\text{MPa}$$

Step 3: Calculation of the axial capacity of a concentrically-loaded column (P_0), flexural strength without an axial force (M_0), and Rankine load (P_R).

The axial capacity of a concentrically-loaded column and flexural moment strength of the column without axial forces can be estimated, respectively, as follows:

$$P_0 = 0.85 f_{ck} A_{reduced} + A_s f_y(T_s) = (0.85 \times 35 \times 38197 + 2042.8 \times 238)/10^3 = 1622.5\text{kN}$$

$$M_0 = A_{s1} f_y(T_s)(d_{s2} - d_{s1}) = 1021.4 \times 238 \times (252.25 - 52.75)/10^6 = 48.5\text{kN} \cdot \text{m}$$

In addition, Rankine load (P_R) is calculated from $1/P_R$=$1/P_0$+$1/P_e$, as follows:

$$P_R = \frac{P_c P_e}{P_c + P_e} = \frac{1622.5 \times 2732.1}{1622.5 + 2732.1} = 1017.97\text{kN}$$

where

$$(EI)_{eff} = 0.25 E_c I_g = 0.25 \times 8500 \sqrt[3]{35+8} \times \frac{200.6^4}{12} = 1{,}004{,}594{,}713{,}123\text{N} \cdot \text{mm}^2$$

$$P_e = \frac{\pi^2 (EI)_{eff}}{(kL)^2} = \frac{\pi^2 \times 1004.594 \times 10^9}{(0.5 \times 3810)^2} \times 10^{-3} = 2732.1\text{kN}$$

Step 4: Determination of the P-M interaction curve without the secondary effect

The coefficients α and β for the simplified P-M interaction curve without considering the secondary effect can be estimated as follows:

$$\alpha = 0.25 \frac{A_g f_{ck}}{A_s f_y} + 0.65 = 0.25 \frac{305^2 \times 35}{2042.8 \times 414} + 0.65 = 1.61$$

$$\beta = -0.4 \frac{A_s f_y}{A_g f_{ck}} + 0.45 = -0.4 \frac{2042.8 \times 414}{305^2 \times 35} + 0.45 = 0.35$$

On this basis, the P-M interaction curve without the consideration of the secondary effect can be calculated, as follows:

$$\text{for } \frac{P_u}{P_0} \geq 0.35 \quad \frac{P_u}{P_0} + 0.4 \frac{M_u}{M_0} = 1$$

$$\text{for } \frac{P_u}{P_0} < 0.35 \quad -1.74 \frac{P_u}{P_0} + \frac{M_u}{M_0} = 1$$

The normalized and simplified P-M interaction curves of the RC column section are shown in Figs. A2(a) and A2(b), respectively.

Step 5: Determination of the P-M interaction curve considering the secondary effect

The coefficients α_2 and β_2 considering the secondary effect can be calculated as follows:

$$\alpha_2 = 3\gamma \frac{A_g f_{ck}}{A_s f_y \frac{kL}{r}} + 0.7 = 3 \times 1 \times \left(\frac{305^2 \times 35}{2042.8 \times 414 \times \frac{0.5 \times 3810}{0.3 \times 305}} \right) + 0.7 = 1.25$$

$$\beta_2 = \beta \frac{P_0}{P_R} = 0.35 \times \frac{1622.5}{1017.97} = 0.56$$

and the normalized P-M interaction curve considering the secondary effect is calculated as follows:

$$\text{for } \frac{P_u}{P_R} = 1 \quad \frac{1}{1.25} \frac{M_u}{M_0} = 1$$

$$\text{for } \frac{P_u}{P_R} < 1 \quad -0.44 \frac{P_u}{P_R} + \frac{M_u}{M_0} = 1$$

This is because P_R=1017.97 kN>P_b(=βP_0)=567.88 kN, and the normalized and simplified P-M interaction curves considering the secondary moment are shown in Figs. A3(a) and A3(b), respectively.

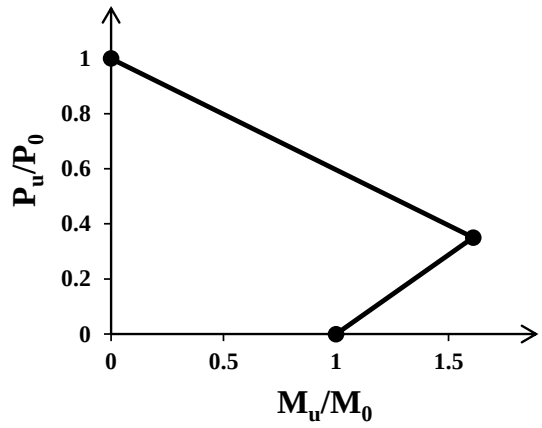

(a) Normalized P-M interaction curve

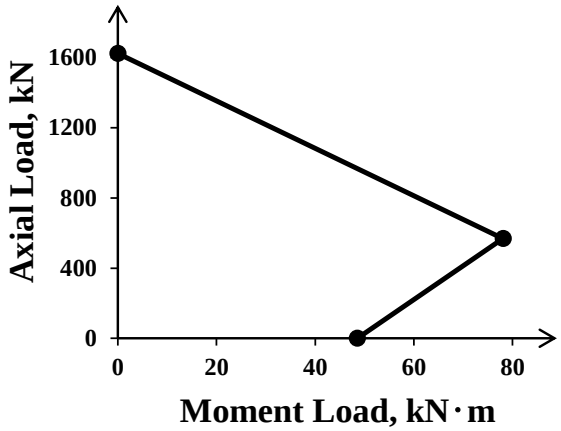

(b) Simplified P-M interaction curve

Fig. A2 Estimated P-M interaction curves without secondary moment effect

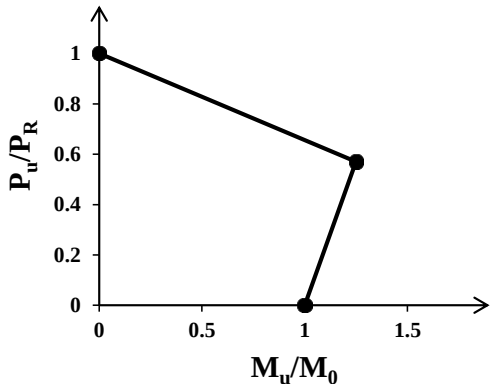

(a) Normalized P-M interaction curve

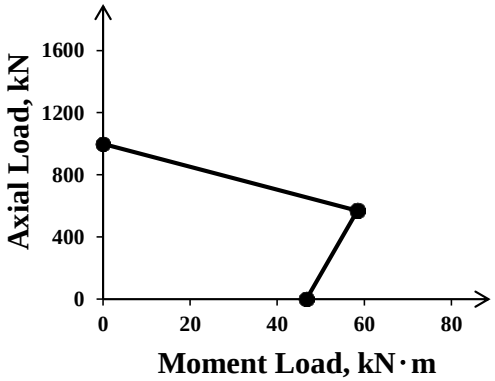

(b) Simplified P-M interaction curve

Fig. A3 Normalized and simplified P-M interaction curves with the secondary moment effect